A&A manuscript no.
(will be inserted by hand later)

Your thesaurus codes are:
13. (02.07.1,02.09.1,05.03.1,11.05.2)

ASTRONOMY
AND
ASTROPHYSICS
5.2.2008

On the stability of motion of *N*-body systems: a geometric approach

A.A. El-Zant[1,2]

[1] Astronomy Centre, University of Sussex, Brighton BN1 9QH, UK
[2] Physics Department, Technion — Israel Institute of Technology, Haifa 32000, Israel

Received .....; accepted.....

Abstract.

Much of standard galaxy dynamics rests on the implicit assumption that the corresponding N-body problem is (near) integrable. This notion although leading to great simplification is by no means a fact. In particular, this assumption is unlikely to be satisfied for systems which display chaotic behaviour which manifests itself on short time-scales and for most initial conditions. It is therefore important to develop and test methods that can characterize this kind of behaviour in realistic situations. We examine here a method, pioneered by Krylov (1950) and first introduced to gravitational systems by Gurzadyan & Savvidy (1984,1986). It involves a metric on the configuration manifold which is then used to find local quantification of the divergence of trajectories and therefore appears to be suitable for short time characterization of chaotic behaviour. We present results of high precision N-body simulations of the dynamics of systems of 231 point particles over a few dynamical times. The Ricci (or mean) curvature is calculated along the trajectories. Once fluctuations due to close encounters are removed this quantity is found to be almost always negative and therefore all systems studied display local instability to random perturbations along their trajectories. However it is found that when significant softening is present the Ricci curvature is no longer negative. This suggests that smoothing significantly changes the structure of the $6N$ phase space of gravitational systems and casts doubts on the continuity of the transition from the large-N limit to the continuum limit. From the value of the negative curvature, evolution time-scales of systems displaying clear instabilities (for example collective instabilities or violent relaxation) are derived. We compare the predictions obtained from these calculations with the time-scales of the observed spatial evolution of the different systems and deduce that this is fairly well described. In all cases the results based on calculations of the scalar curvature qualitatively agree. These results suggest that future applications of these methods to realistic systems may be useful in characterizing their stability properties. One has to be careful however in relating the time-scales obtained to the time-scales of energy relaxation since different dynamical quantities may relax at different rates.

Key words: Gravitation – Instabilities – Celestial mechanics, stellar dynamics – Galaxies: evolution

1. Introduction and motivation

1.1. On the assumptions of standard galaxy dynamics

The classical assumption often made in galaxy dynamics (Binney & Tremaine 1987 (BT) chapter 4) is that present day galaxies can be treated as collisionless fluids in steady states described by one particle distribution functions obeying the time independent collisionless Boltzmann equation (CBE). In addition, it is often supposed that these distribution functions are completely characterized by the isolating integrals of motion (of single stars).

implies that almost all orbits are regular and therefore stars conserve as many integrals of motion (in involution) as the number of spatial dimensions they move in. Thus, for a three dimensional system of N stars there are $3N$ conserved quantities and the N-body problem is solvable by quadratures—or integrable (see e.g., Whittaker 1937 or Goldstein 1980 for discussions using classical analysis: more modern treatments can be found in Arnold 1989 (ARN) or Abraham & Marsden 1978).

Thus in this picture galaxies are modeled as classical fluids with time independent densities which give rise to potentials similar to those for which the Hamilton-Jacobi equation is separable. Obviously these assumptions cannot be strictly satisfied for real galaxies. It is argued however, that due to the large two body relaxation time (e.g., Saslaw 1985)

$$\tau_b = \frac{v^3}{32\pi G^2 m^2 n \ln(N/2)} \qquad (1)$$

(where v is the characteristic speed of a star and n is the number density of "field stars" of mass m) that these systems can be treated as effectively collisionless over many Hubble times. However all that Eq. (1) is saying is that the direct impulse from encounters between pairs of stars is small relative to the velocity of a star in the smoothed potential. This is due to the long range nature of gravitational interactions which ensures that the whole system contributes to the mean force on a star at all times. In the approximation leading to (1) however the perturbation to the trajectory of a test star due to a certain field star is only calculated at their closest approach — that is only once during a crossing time. Nevertheless, due to the complicated nature of the solutions of the Newtonian equations for $N > 2$, discreteness can have a major indirect effect; the nonlinearity of the problem prevents the adding up of the motions due to individual binary interactions to each other and to

the motion in the mean field since although the forces add up linearly the solutions of the Newtonian equations do not. This suggests that the N-body problem is perhaps best studied in its entirety. In this regard it may be perhaps useful to recall that the collisionless steady-state approximation is not a trivial simplification of the dynamics: It reduces the N-body problem to N one-particle problems in a given potential, thus reducing the number of coupled first order differential equations to be solved from $6N$ equations to 6 equations.

For general Hamiltonian dynamical systems, regular motions form invariant (under time propagation of the solution) tori in the $6N$ phase-space. In integrable systems these occupy the whole of that space. Under perturbations, however, some tori are destroyed leaving behind volumes of phase space where irregular (or chaotic) motion can occur. The extent of the chaotic region will depend on the strength of the perturbation. Bounds given by the KAM theorem predict that a positive measure of tori will survive provided the perturbation to the potential $\mu < \mu_c$, where μ_c is a critical amplitude (e.g., Mackay & Meiss 1987). In general, the value of μ_c decreases as $\exp(-N \log N)$ and has been shown to be irrelevant for many higher dimensional physical systems (Pettini 1993 (P93) and the references therein) while the perturbation due to discreteness noise decreases only as $1/\sqrt{N}$ if it is random (e.g., Saslaw 1985). The diffusion time away from the remaining tori is also a decreasing function of N; $\tau_D \sim \exp(1/\mu)^{1/N}$ (Nekhoroshev 1977; Perry & Wiggins 1994). These results suggest that a system is unlikely to become more regular with increasing N, in direct contradiction with the results of two body relaxation estimates but as expected from considering the complicated nature of solutions of generic N-body systems. In fact, for the particular case of a spherical gravitational system, it was shown by Gurzadyan & Savvidy (1986) (GS) that as N increases this system tends towards an Anosov (1967) C-system with maximal instability in phase-space (if one neglects escapes and direct collisions). Making the same kind of assumptions as those used to obtain Eq. (1) (by considering an infinite and homogeneous medium), GS obtain the following relation for the N-body relaxation time arising from the instability

$$\tau_{gs} = (15/4)^{2/3} \frac{1}{2\pi\sqrt{2}} \frac{v}{Gmn^{2/3}}. \quad (2)$$

which is considerably shorter than the binary relaxation time.

C-systems are very irregular — to the point that their evolution can be described as a Markow process (e.g., Pesin 1989). The collisionless approximation however predicts that spherical systems end up in completely integrable steady states — the most regular and predictable systems that can exist. The contradiction can possibly arise because the analysis leading to (1) focuses on the fact that the force function becomes smoother as N increases. It then assumes directly that this implies the solution becoming more regular not taking into account that exponentially smaller perturbations are sufficient with increasing N to make an N-body system unstable. Therefore, while some quantities that do not depend on the exact details of the dynamics may be slowly evolving and not sensitively dependent on the discreteness noise, the solutions themselves are heavily sensitive to noise. For example, the change in the energies of stars that arises from discreteness noise is likely to be much slower than the changes in their trajectories. A rough example is the fact that numerically integrated orbits in fixed (and smooth) potentials can have the energy (and all the Poincaré invariants) conserved along their trajectories to up to ten digits while the trajectories themselves are completely inaccurate perhaps not resembling (even qualitatively) the real ones (El-Zant 1996b). The numerical errors here represent the noise (if they are taken to be random, a proposition still under discussion: McCauley 1993). This is because here energy is a scalar function of the phase space variables and is related to the force by a path independent integral. That path on the other hand is a 6 component vector in phase space. One can thus easilly envisage perturbations that change the trajectory of a particle without changing its energy. A long time-scale of energy relaxation does not therefore imply that the actual detailed dynamics are collisionless in the sense of being stable solutions of the CBE. One would expect that some macroscopic quantities could be affected, for example velocity dispersion or the actual shape of the gravitational system.

In fact, simulations of single particle motions in fixed potentials show that the time-averaged phase-space density distribution of individual chaotic trajectories, as well as their statistical properties, change significantly over a time-scale $\ll \tau_b$ when the potential is given some graininess (Pfenniger 1986; Udry & Pfenniger 1988), or when the trajectories are given small random kicks without changing their total energies significantly (Kandrup 1994; Merritt & Valluri 1996; El-Zant 1996b). The full N-body problem would be expected to be much more irregular and prone to evolution on small (compared to τ_b) time-scales. Such effects are actually observed in N-body simulations of up to 10^6 heavily softened particles but are assumed to be due to the relatively small number of particles present, even though the two body relaxation time in these simulations is still usually much larger than the time-scales considered. (a review of such occurrences is given by Hernquist & Ostriker 1992: see also van Albada 1986; Sellwood 1987: Zhang 1996 presents a detailed study of an example of a case where discreteness noise interacts with global irregularities in the density thus triggering evolution). In addition, processes involving non-stellar objects such as interactions with giant molecular clouds in galactic disks or black holes in halos, small dissipative perturbations (e.g., Pfenniger & Norman 1990) etc. can cause even more serious trouble for the collisionless approximation.

Even if the collisionless approximation does hold, this does not guarantee that a given density distribution would not evolve over a Hubble time. This is because individual trajectories, even in a smooth steady-state potential, can have time dependent density distributions over such a time-scale. This would be the case in general non-spherical potentials as noted by Binney (1982). Hasan et al. (1993) describe such behaviour for barred spirals while Merritt & Fridman (1996) show that it may also be important for ellipticals. El-Zant (1996b) examines the case of trajectories started near the symmetry plane of disks embedded in triaxial halos. Finally, it seems that perhaps there is also some observational evidence for evolutionary phenomena occuring in galaxies (Wielen 1977; Pfenniger et al. 1994; Courteau et al. 1996; Pucacco 1992).

The above considerations suggest (although in no way prove) that even though gravitational systems obey the CBE in the infinite N limit (e.g., Braun & Hepp 1977) the existence and stability (against discreteness noise) of steady state solutions of that equation are in question when a significant amount of chaos is present. This means that while in some cases the classical theory may still hold over a few Gyr (considering the primitive evolutionary state of cold disks in some

spiral galaxies one has to admit that this could often be the case) it does not always obviously do so.

1.2. How chaos drives evolution

A distribution of stars giving rise to an integrable potential can either oscillate coherently or reach a macroscopic steady state through phase mixing. This is a trivial form of relaxation which is simply due to stars moving at different angular frequencies on their respective KAM tori in the 6-dimensional phase-space — the motion in the $6N$-dimensional phase-space being a $3N$ torus characterized by the $3N$ integrals. Phase mixing conserves the action variables characterising this torus and which are crucial in determining the physical state of a system. Most galaxies are not believed to be undergoing significant large scale oscillations, we therefore conclude that if they are integrable dynamical systems they must be in a steady state. Moreover, if they are sufficiently far from any chaotic system they must be stable to small perturbations (KAM theory). This is what is assumed in the classical theory.

A necessary condition for evolution therefore is the non-integrability of the system. This condition is satisfied for N-body gravitational systems since there are no global integrals of motion other than the classical ones (Poincaré 1889). However, not all non-integrable systems exhibit interesting behaviour (different from classical theory) in the time-scales of interest. We need the property of *phase-space* mixing — that is the spread of localized volume elements (corresponding to sets of initial conditions) to cover large areas of the $6N$ phase-space (while still conserving their original Lebesgue measure: e.g., Sagdeev et al. 1988). Phase-space mixing leads to diffusion in the action variables and may therefore lead to evolution in a system's physical parameters. For this process to be efficient it is necessary that the system be sufficiently chaotic so that the diffusion occurs over short enough time-scales and covers a large range of initial states, only then can we say that the macroscopic state corresponding to a given set of micro-states can evolve over a Hubble time.

It is therefore important to examine different methods for detecting these processes and the time-scales associated with them in practical situations where the predictions can be tested. The rest of this study is a step in this direction. In the next section we describe why certain subtleties related to N-body gravitational systems require *local* methods to be used in the quantification of chaotic behaviour. One such approach based on the geometry of the configuration manifold is then described. In section 3 we describe some of the possible applications of this approach while in section 4 results of some numerical experiments testing the method are reported.

2. Characterization of chaos and the Ricci criterion

2.1. Difficulties with commonly used methods

Central to the idea of phase-space mixing is the concept of dynamical entropy used to quantify it. The most important of such quantities is the so called Kolmogorov-Sinai entropy. The easiest way of calculating the KS entropy is by evaluating the Liapunov exponents, which for a dynamical system defined by the vector equations

$$\dot{\mathbf{X}} = \mathbf{F}(\mathbf{X}), \tag{3}$$

with solution $\bar{\mathbf{X}} = \bar{\mathbf{X}}(t, t_o, \bar{\mathbf{X}}_\mathbf{o})$ are given by

$$\sigma(\boldsymbol{\xi_0}, \boldsymbol{X_0}) = \lim_{t\to\infty} \frac{1}{t} \log \frac{\parallel \boldsymbol{\xi}(t) \parallel}{\parallel \boldsymbol{\xi}(0) \parallel}, \tag{4}$$

where $\boldsymbol{\xi}$ is a tangent space vector arising from the solution of the variational equations

$$\dot{\boldsymbol{\xi}} = \mathbf{D_x F}\left(\bar{\mathbf{X}}\left(t, t_o, \mathbf{X_o}\right)\right) \boldsymbol{\xi}. \tag{5}$$

The KS entropy is then usually given by (e.g., LL)

$$KS = \int \sum_i \boldsymbol{\sigma}(\boldsymbol{\xi}^i, \boldsymbol{X}_o) d\mathbf{X_o}, \tag{6}$$

where the sum is taken over all positive exponents and the integral is over all possible initial conditions. For systems with simple enough phase-space and when the infinite time characteristics are required, the KS entropy calculated with the help of this formula suffices to describe the ergodic properties of a system. Positive KS entropy over a compact phase-space, or some region of it that has this property, is a sufficient condition for the presence of what is usually called chaos and the accompanying erratic behaviour which leads to the approach towards statistical equilibrium even in low dimensional systems (e.g., McCauley 1993). The evolution time-scale is usually related to the inverse of the KS entropy.

Open systems interacting via un-softened Newtonian potentials do not have compact phase-spaces however, and therefore the situation is more complicated. Here, no final state exists and one has to distinguish between the various stages of evolution i) Violent relaxation, ii) Collective (plasma type) instabilities iii) Evolution towards an isotropic rotator and iv) Kinetic evolution towards equipartition of energy, core collapse etc. Here, the distinctions are rather arbitrary and are used only for clarity — these processes may interact and influence each other. Stage three has been given very little attention in the literature because of the lack of a mechanism from traditional physics leading to such evolution (on a time-scale smaller than given by (1)). Nevertheless, the chaotic nature of the N-body problem may provide a clue as to how this might happen.

All the above processes should be characterized by phase-space instability leading to mixing, but evidently cannot be described by any quantities defined only for infinite times. One way out of this problem is to integrate either the linearized equations (5) (e.g., Goodman et al. 1993) or the full non-linear equations (3) for slightly different initial conditions (e.g., Kandrup et al. 1994 and the references therein) for short times. One drawback of such an approach, however, is that one is comparing the divergence in phase-space of different temporal states and not trajectories. Integrable systems usually have linear (in time) phase-space divergence between neighbouring states — but *only on average*. A simple illustration of the type of problems involved is provided by examining the behaviour of a pendulum

$$\ddot{\theta} = -\sin\theta, \tag{7}$$

with linearized equation

$$\delta\ddot{\theta} = -\cos\theta\delta\theta. \tag{8}$$

When $\cos\theta$ is negative this has a solution

$$\delta\theta \sim e^t. \tag{9}$$

That is, during this interval, the solution of the linearized equation predicts "exponential instability". Obviously, in this example, the trajectories do not diverge at all — but the states did. In addition, methods that evaluate the whole set of Liapunov exponents of a dynamical system are fairly sophisticated (e.g., Eckmann & Ruelle 1985) and are not practical for higher dimensional systems. This in practice will mean that one will have to evaluate only the largest exponent which is a measure of the maximal instability in phase-space. Now, in a multidimensional separable system it is likely that at any given time there will be some oscillations that are in the "$\cos\theta < 0$ region" — that is displaying exponential divergence in the linearized dynamics. An initial randomly oriented vector in the linear tangent space will always reorient itself along the direction of maximum expansion under the stretching effect of the flow (e.g., Wolf et al. 1985). It could therefore be possible to obtain average exponential divergence in the linearized dynamics even for separable systems. This approach therefore may be unable to distinguish between genuine phase space mixing leading to evolution and trivial phase mixing of temporal states. It may also be useful to note here that there are few strict results concerning the properties of the Liapunov exponents for higher dimensional systems (Eckmann & Ruelle 1985; Pesin 1989).

2.2. The study of motion on Lagrangian manifolds

There are a variety of ways of transforming Hamiltonian problems into the study of some metric space (see P93; Gurzadyan & Kocharyan 1994 or the articles by Gurzadyan and Pettini in Gurzadyan & Pfenniger 1994). The oldest and most well known of these hinges on the observation, apparently first made by Hertz (1900) in the course of his remarkable reformulation of classical mechanics, that the Maupertuis principle

$$\delta \int_{\gamma} 2T dt = 0, \tag{10}$$

(where T is the kinetic energy along the motion on a trajectory γ) from which the equations of motion in their Lagrangian form arise is actually an expression for geodesics on a the configuration manifold M where the motion is restricted as a result of conservation laws. The fact that (10) defines geodesics is clear from the following relations:

$$\delta_e \int T dt = \delta_e \int \sqrt{T}\sqrt{T} dt = \delta_e \int \sqrt{T} dl = \delta_e \int \sqrt{E-V} dl, \tag{11}$$

where $E = T + V$ is the total energy and $dl = \sqrt{a_{ij} dq^{ij}}$ with

$$T = a_{ij} \frac{dq^i}{dt} \frac{dq^j}{dt} \tag{12}$$

for particles of unit mass. Here the a_{ij} are elements of the metric tensor and δ_e refers to variations in the trajectory γ holding the energy and the end points fixed. These are thus geodesics in the energy sub-manifold of the configuration space and the q^i are coordinates on it. If we now choose Cartesian coordinates in the enveloping $3N$ space then

$$dl^2 = \sum (dx^{\alpha})^2. \tag{13}$$

The metric then is

$$ds^2 = (E - V) \sum_{3N} (dx^{\alpha})^2 . \tag{14}$$

From the Jacobi equation which describes the geodesic deviation on M (e.g., Misner et al. 1973)

$$\nabla_{\mathbf{u}} \nabla_{\mathbf{u}} \mathbf{n} + \mathbf{Riem}(\mathbf{n}, \mathbf{u})\mathbf{u} = \mathbf{0}, \tag{15}$$

(where $\mathbf{n}$ is a separation vector analogous to $\boldsymbol{\xi}$ in (4), **Riem** is the Riemann curvature operator, and $\nabla_{\mathbf{u}}$ the covariant derivative) one can obtain the following relation for the norm of the *normal* component of this deviation

$$\frac{d^2 \parallel \mathbf{n} \parallel^2}{ds^2} = -2k_{\mathbf{u},\mathbf{n}} \parallel \mathbf{n} \parallel^2 + 2 \parallel \nabla_{\mathbf{u}} \mathbf{n} \parallel, \tag{16}$$

where

$$k_{\mathbf{u},\mathbf{n}} = \frac{[\mathbf{Riem}(\mathbf{n}, \mathbf{u})\mathbf{u}] . \mathbf{n}}{\parallel \mathbf{n} \parallel} \tag{17}$$

is the two dimensional curvature in a plane defined by $\mathbf{u} \times \mathbf{n}$ and where we have used the fact that $\mathbf{n}_{\perp} . \mathbf{u} = \mathbf{0}$. If $k_{\mathbf{u},\mathbf{n}}$ is negative everywhere for all planes as defined above (that is for all $\mathbf{n}$ normal to $\mathbf{u}$) and if $-k = \min \mid k_{\mathbf{n},\mathbf{u}} \mid$ we have

$$\parallel \mathbf{n}(s) \parallel \geq \frac{1}{2} \parallel \mathbf{n} \parallel \exp \sqrt{-2k} s \tag{18}$$

for $\dot{\mathbf{n}} > \mathbf{0}$, and

$$\parallel \mathbf{n}(s) \parallel \leq \frac{1}{2} \parallel \mathbf{n} \parallel \exp -\sqrt{-2k} s, \tag{19}$$

for $\dot{\mathbf{n}} < \mathbf{0}$. These relations describe the linearized dynamics in the "dilating" and "contracting" spaces characteristic of the class of Anosov (1967) C-systems to which, as was mentioned earlier, large spherical N-body systems belong. In this case, $\sqrt{-\sum k_{\mathbf{u},\mathbf{n}}}$ averaged over M is the KS entropy. In comparing two C-systems therefore one can *define the system with larger average value of* $\sqrt{-\sum k_{\mathbf{u},\mathbf{n}}}$ *to be more unstable*. This system will have a larger exponentiation rate and so initial conditions will tend to mix faster along geodesics. To determine how fast the initial conditions mix in time, we note that $ds/dt = \sqrt{2}T$ so that if T does not vary too much during the evolution $s \sim \sqrt{2}Tt$. It is clear that a system with the above characteristics cannot conserve its action variables since there is always a deviation of trajectories normal to the motion in phase-space (which is the cotangent bundle of M).

2.3. Ricci curvature and the corresponding criterion

GS have shown that the condition for C-systems is not satisfied for general gravitational ones. However, as Kandrup (1990a,1990b) has shown, the probability of a two dimensional curvature being positive along a N-body system's trajectory decreases exponentially with increasing N. Also, in the N-body problem relation (18) implies that all orbits are unstable at all times. However, one needs much less than what is described by (18) for observable effects of instability to be detected (just 10% of orbit becoming unstable may be enough). On the other hand, just a few orbits being unstable in general would not significantly change the physical properties of a system. We therefore need some averaged form of (16) and a

corresponding instability relation instead of (18) to characterize such behaviour. Ideally such a relation should not require the evaluation of the Riemann tensor.

A natural way of proceeding is by using the Ricci (or mean) curvature of the manifold M

$$r_{\mathbf{u}}(s) = R_{ij}\frac{u^i u^j}{\parallel \mathbf{u} \parallel^{\mathbf{2}}}, \tag{20}$$

where R_{ij} are elements of the Ricci tensor and $u^i = \frac{dx^i}{ds}$ are the components of the geodesic velocity vector $\mathbf{u}$. The Ricci curvature is related to the two dimensional curvatures by (Eisenhart 1926)

$$r_{\mathbf{u}} = \sum_{\mu=1}^{3N-1} k_{\mathbf{n}_\mu,\mathbf{u}}(s). \tag{21}$$

The value of $r_{\mathbf{u}}$ does not depend on the particular set of normal directions $\mathbf{n}$ chosen so that $r_{\mathbf{u}}/(3N-1)$ can be seen as the average value of $k_{\mathbf{u},\mathbf{n}}$ over all possible directions normal to $\mathbf{u}$ on the configuration manifold M.

In the case when all k's are negative, $\sqrt{-r_u}$ averaged over the whole manifold corresponds to the Kolmogorov entropy. In general, as was first noted by Gurzadyan & Kocharyan (1987), it will provide an "averaged" measure of irregularity. In these terms Equation (16) can be written as

$$\frac{d^2Z^2}{ds^2} = -2\left[\frac{r_{\mathbf{u}}(s)}{(3N-1)}\right]Z^2 + 2\langle \parallel \nabla_{\mathbf{u}}\mathbf{n} \parallel\rangle, \tag{22}$$

where Z is now to be interpreted as the norm of a vector that is a member of a random field of vectors with uniform distribution in directions normal to $\mathbf{u}$ and equal magnitude (El-Zant 1996a).

If $r_{\mathbf{u}}(s)$ is negative on a region of M then one can obtain relations for Z analogous to those obtained for $\parallel \mathbf{n} \parallel^{\mathbf{2}}$ in (18) with $-k_r = \frac{\min[r_{\mathbf{u}}(s)]}{3N-1}$. One can then apply the criterion of relative instability of C-systems to general Hamiltonian dynamical systems in regions of their configuration manifolds where the Ricci curvatures are negative, which in this case will express the relative probability of any two systems being unstable under random perturbations. We adopt here the following definition, convenient for numerical studies of N-body systems.

Definition:
Let R_1 be some subset of the configuration manifold M_1 and R_2 be a subset of a manifold M_2 with M_2 not necessarily different from M_1. Suppose also that the Ricci curvature is negative in both of these regions. *We will say that R_1 corresponds to configurations of a dynamical system that are more unstable than those represented by R_2 if the average value of $\sqrt{-r_{\mathbf{u}}}$ is larger in R_1 than in R_2.*

Note that: As in the case of C-systems we obtain time-scales from the relation $\frac{ds}{dt} = \sqrt{2}T$. If we are comparing systems with different kinetic energies, the evolutionary times derived will have to be scaled accordingly. If the kinetic energies of systems are changing in the region of the dynamical systems of interest then time-scales derived from the Ricci curvature alone are not rigorous. If the logarithmic time derivative of the kinetic energy is small however then $s \sim \bar{T}t$ (where the bar denotes an average over the region of interest). Otherwise a fully dynamical formulation with time replacing s in Equation (22) would have to be considered (P93; Cerruti-Sola & Pettini 1995). The latter approach would also have to be used if the curvature on M is not predominantly negative. Also if the systems we are comparing consist of different numbers of particles, $r_{\mathbf{u}}$ will have to be divided by $3N-1$.

The definition leaves us the choice to compare different areas of the manifold of the same dynamical system, or those of different systems. Also the averages can either be static, or taken along a computed trajectory of the system. Since the regions R in the definition above can be taken as small as we wish, the method is clearly local. This is possible because $r_{\mathbf{u}}$ is directly related to the local geometry of the manifold where a system lives and is not an asymptotic quantity. Also, although the above formulation does not allow explicitly for dissipative forces, these can be added as time dependent perturbation to an open Hamiltonian system.

To actually calculate the value of $r_{\mathbf{u}}$, one contracts the Riemann tensor (which for the metric (14) is given in GS) and uses (20) to obtain

$$r_u = 3A\frac{\left(W_i u^i\right)^2}{W^2} - 2A\frac{W_{ij}u^i u^j}{W} - \left(A-\frac{1}{2}\right)\frac{\parallel \nabla W \parallel^2}{W^3} - \frac{\nabla^2 W}{2W^2} \tag{23}$$

with $A = \frac{3N-2}{4}$. Here W denotes $T = T(V)$ while ∇W and $\nabla^2 W$ represent its Cartesian gradient and Laplacian respectively. From the metric (14) one can deduce that $u^i = \frac{dx^i/dt}{\sqrt{2}W}$ and $\parallel \mathbf{u} \parallel = 1$. For an N-body system, the implied summation would be over $i, j = 1, 3N$. Moreover, if the interactions proceed through the usual Newtonian law with no direct impacts $\nabla^2 W = 0$. If we now label by a, b and c the particle numbers (which run from 1 to N) and by k and l the three Cartesian coordinates of a particle, it is straightforward to obtain the following expressions for the derivatives of W

$$W_i = \frac{\partial W}{\partial x_i} = \frac{\partial W}{\partial r_a^k} = -\sum_{c\neq a}\frac{r_{ac}^k}{r_{ac}^3}, \tag{24}$$

$$W_{ij} = \frac{\partial^2 W}{\partial x_i \partial x_j} = \frac{\partial^2 W}{\partial r_b^k \partial r_a^l} = \left[\frac{\delta_{kl}}{r_{ab}^3} - \frac{3r_{ab}^k r_{ab}^l}{r_{ab}^5}\right], \tag{25}$$

if $a \neq b$ and

$$W_{ij} = \frac{\partial^2 W}{\partial x_i \partial x_j} = \frac{\partial^2 W}{\partial r_b^k \partial r_a^l} = -\sum_{c\neq a}\left[\frac{\delta_{kl}}{r_{ac}^3} - \frac{3r_{ac}^k r_{ac}^l}{r_{ac}^5}\right], \tag{26}$$

if $a = b$. In these equations

$$r_{ab}^2 = (r_{ab}^1)^2 + (r_{ab}^2)^2 + (r_{ab}^3)^2 \tag{27}$$

and $\quad r_{ab}^k = r_a^k - r_b^k$.

The practical procedure of implementing the criterion described above will therefore consist of using the position and velocities of particles for the configurations of the system under study to obtain $\mathbf{u}$, W, and the quantities defined in (25). These are substituted into (23) to find $r_{\mathbf{u}}$. In this way, one can calculate the Ricci curvature for various regions of the configuration manifolds of different systems. If the Ricci curvature is found to be predominantly negative, we then use the above definition to classify systems according to their local stability properties.

There are many advantages to the above setup. For example, what is studied here is the normal deviation due *random* perturbations of trajectories with the same geodesic velocities

$\| \mathbf{u} \| = 1$ on M and not the deviation of temporal states in the direction of maximal growth. Therefore what can be termed the 'chaotic pendulum problem' is avoided. In fact, it can be seen from (23) that all systems possessing only one degree of freedom (those with $3N = 1$) have an $r_{\mathbf{u}} = 0$ at all times. In the terminology of classical stability theory it is said that the negativity of the Ricci curvature measures the orbital stability as opposed to the more strict Liapunov stability (Pars 1965). Because of these properties the Ricci curvature is unlikely to be negative for multidimensional integrable systems in virial equilibrium. This assertion has been checked for the special case of the two body problem with circular orbits (where the virial relation is satisfied) but obviously needs further investigation. For a system in a full statistical quasi-steady state a negative Ricci curvature must mean that the system is chaotic and mixing for all initial conditions since $r_{\mathbf{u}}$ is constant for systems in a steady state. However, in general, the negativity of the Ricci curvature on most of a system's trajectory does not guaranty that it is chaotic but only that there is a probability of this being the case (the probability increasing with the fraction of time spent in the negative region).

Other advantages of this method are that the integration of a large number of linearized equations is avoided and space averages on compact manifolds can be compared to time averages (e.g., Casetti & Pettini 1993), thus allowing one to check for properties such as ergodicity for single particle orbits and specially constructed N-body systems for which M is compact (such as those consisting of softened particles enclosed enclosed in boxes: e.g., Lynden-Bell 1972).

3. Applications

3.1. Some applications that take advantage of the geometric setting

There are at least three applications that can make use of the geometric method described above.

1. Studying the instability properties of individual orbits in fixed potentials with compact phase-spaces (in this case the formulas in (25) will, of course, have to be modified accordingly).
2. Since $r_{\mathbf{u}}$ in Eq. (23) depends only on functions that are given by sums over the particle positions and velocities, it is constant (up to $1/\sqrt{N}$ fluctuations) for systems in statistical equilibrium. In this case, it is therefore possible to replace time averages with phase-space averages (that is different realization of same density and velocity fields). This time however the averages are made over the full $6N$ phase-space. The Ricci curvature therefore would give us a powerful tool of exploring that space at and around equilibrium solutions. Important questions such as the degree of chaos in a system, mixing time-scales, and the variation of these properties with particle numbers can then be tackled in the $6N$ phase-space without making assumptions about the particle particle correlations. It is very important to compare such predictions with those of single particle integrations in fixed potentials to evaluate the role of discreteness in the evolution of gravitational systems. For as we shall see in the next section, systems with large softening parameters appear to have very different $6N$ phase-space structures compared to those composed of point particles.
3. One can apply the method directly to the results of N-body simulations. The formula for calculating the Ricci curvature should be easily incorporated into large-N codes such as the TREECODE. This would help in interpreting the results of N-body simulations and lead to classification of galaxies according to their dynamical instability properties. Moreover, one can then study the direction of evolution of instability properties of realistic gravitational systems. For example it has been argued by Gerhard (1985) that elliptical galaxies start from chaotic states and evolve towards progressively more regular states which are then for long times indistinguishable from those of integrable systems. An alternative scenario is closer to the conventional dynamical interpretation of statistical mechanics. In this picture, a quasi-steady state is achieved when a system, although highly mixing, keeps its macroscopic parameters constant and is stable against perturbations to its statistical properties. The point being that, if the instability is present for most initial conditions of interest (that is if we have constant negative $r_{\mathbf{u}}$ for long enough times), that would mean that the system is free to move in the region of interest and will tend towards a more probable state. This state would (by definition) contain more microscopic states compatible with it and the system would be free to move between them. This situation is more compatible with the interpretation of violent relaxation as leading to most probable end states compatible with a set of constraints (Saslaw 1985) since regular states cannot be very probable because they lie on $3N$ subspaces of the $6N - c$ dimensional subset of the phase-space where all possible states live ($c = 10$ stands for the number of classical integrals used in the reduction of the N-body problem, e.g., Whittaker 1937).

3.2. Specific application and model parameters

As a first test we apply the method described above to small N-body systems of 231 point particles. The small number enables us to integrate the equations of motion with high precision, on the other hand the number should be sufficient for the results to have some statistical significance. It is essential to check if the Ricci curvature method makes adequate predictions about the evolution of gravitational systems under these controlled conditions before applying it to realistic galaxy models where a host of auxiliary problems will arise. The small numbers however makes it harder to distinguish clearly between the predictions of the Ricci method and those of two body relaxation theory. A detailed comparison (including dependence of the results on N) is better left to another study.

We choose initial conditions in which the particles are arrayed into two sheets. An upper one with 11 lines consisting of 11 particles each and a lower one composed of 11 lines with 10 particles each. The lines of the upper and lower sheets are positioned in such a way that a line in the lower sheet lies at half the distance (in the plane of the sheet) between two lines in the upper sheet, so as to avoid direct contact of particles from two different sheets when the system evolves. The separation between the two sheets is taken to be equal to half the separation between lines in the same sheet (see the $t = 0$ snapshots in Fig. 3 for example). Such configurations are artificial and are therefore likely to quickly and visibly evolve, hence saving us the trouble of long time integrations.

We use units in which the gravitational constant is unity, the masses of all particles are also taken as unity. Time in these units will be referred to as "physical time". Three scales

are used to determine the separation between adjacent particles $d = 100 \times Scale$, where $Scale$ takes either the value of 1, 10.8 or 100. In what we may call the "main models" we give the initial configurations a rigid body rotation corresponding to an angular momentum of 44275 units around the Z-axis (with zero initial velocities in the Z direction), or a random number generator is used to fix the X-Y velocities which give rise to a small angular momentum of 62.61 units. The three cases of $Scale = (1, 10.8, 100)$ correspond to energies of $(-41.471, -5.705, -0.635)$ with corresponding initial virial ratios of $(0.695, 0.0644, 0.00695)$ respectively. Alternatively, some runs are started with a fixed initial virial ratio of 1 and with the same energies as above. The angular momentum is adjusted accordingly. We shall call these the "equilibrium models" although they do not start from a detailed dynamical equilibrium.

The integrations are performed using a variable order variable step size Adams method as implemented in the NAG routine D02CBF using a tolerance of 10^{-13}. The energy is accordingly conserved to better than 10 digits (usually 12) for a few dynamical times. This accuracy is necessary for a first numerical test to eliminate the factor of serious numerical error from the interpretations of the results. For the same reason we integrate the equations for a relatively short time of about four and a half dynamical times (τ_D =(mean density)$^{-1/2}$), $4.24\tau_D \sim \tau_b$) corresponding to about 2200 time units for the $scale = 1$ case (in a few cases we have performed longer time integrations). The un-softened force law is used, and softening is only introduced to study its effect.

4. Results of numerical experiments

4.1. Averaging

In order that our criterion may be useful, the Ricci curvature must remain mostly negative throughout the evolution of a given system. This condition cannot be generally satisfied because $r_{\mathbf{u}}$, as given by (23), is singular as $r_{ab} \to 0$ for any a and b. The time for which r_{ab} is near zero must also be small compared to the dynamical time-scale of the system (a bounded circular orbit of two particles of separation 0.1 has a period of $\sim 2 \times 10^{-4}\tau_D$ with τ_D the dynamical time of the $Scale = 1$ main model). Therefore, during an encounter of two or more point masses, their contribution will fluctuate violently and dominate $r_{\mathbf{u}}$, this contribution will have a positive average since for a time it mimics that of a two body system. Thus we expect $r_{\mathbf{u}}$ to be a very "bumpy" function of time for N-body systems of point particles. This is indeed the case, as we can see from Fig. 1A, where the Ricci curvature is plotted as a function of dynamical time for the rotating main model with $Scale = 1$ (see section 3.2). We will therefore have to try to eliminate this bumpiness in the hope that the residual curvature is negative if the system is mixing. The approach we will use here hinges on a theorem by Bogoliubov (P93 and the references therein) which states that for equations of the type (22) averaged over small time-scales, the solution is similar to that of the original equation averaged over that time-scale if one excludes the possibility of parametric instability (e.g., ARN) and direct singularities; this is the method we try in this study. We will not attempt here to find out what the theoretically optimum way of doing that should be, but will proceed empirically. As a first approach we will just average over a time-scale containing many "bumps" but still small compared to the total integration time.

Fig. 1B shows the time series in Fig. 1A averaged over steps of $(1/100) \times 4.4\tau_D$ (corresponding to 22 data points in Fig 1A) we see that now the series becomes much more regular. To make further progress we remove the contributions from the most extreme peaks which can dominate the average giving misleading results (these peaks represent points nearer to singularities). It is clear from Fig. 1A that peaks with absolute values larger than $2-4\times10^{-4}$ are rare and isolated, one therefore is tempted to filter the results so as not to include in the calculation of the average any peaks larger than a threshold of this order of magnitude. Fig. 1C shows the behaviour of $r_{\mathbf{u}}$ when a threshold of 2×10^{-4} is taken. The striking result is the apparent regularity and negativity of the Ricci curvature in this case.

It is now important to check that these results do not sensitively depend on the values of the threshold used or the averaging interval taken. Fig. 1D shows the behaviour of $r_{\mathbf{u}}$ when a threshold of 4×10^{-4} and 10×10^{-4} (instead of 2×10^{-4}) is used. The results clearly appear to be qualitatively similar. Indeed, it has been found that the results start to become radically different only for a threshold $\sim 20\times10^{-4}$. Unless stated otherwise, it is implied that it has been checked that the results do not sensitively depend on the threshold taken and that a value of 2×10^{-4} has been adopted. It has also been checked that the results do not sensitively depend on the size of the subdivision intervals (as long as they are not too small of course). We will take averages over a hundred subdivisions of the integration interval unless otherwise stated.

4.2. Rotating versus Non-rotating models

Rotation, plays a central role in stellar dynamics and is one of the parameters that vary along the Hubble sequence. Intuitively, systems where random motion dominates are expected to mix faster (at least initially) than ones where ordered rotational motion does. Observations of elliptical galaxies also show them to be highly mixed and relatively (in comparison with spirals) relaxed objects so that an effective mixing mechanism must have been at work at some stage (and could still be). Our first application will therefore be the comparison of a rapidly rotating system to one without (almost) any rotation.

In Fig. 2 we have plotted the time series of $r_{\mathbf{u}}$ for the two main models with $Scale = 1$. Shown by the solid line is the series corresponding to the random initial velocities, while the dotted line represents the evolution of $r_{\mathbf{u}}$ for the rotating case. Initially, the random system is much more unstable as expected, while later on it starts evolving on a longer time-scale (characterized by the small $r_{\mathbf{u}}$) while the reverse is true for the rotating system.

Explanation of this behaviour of $r_{\mathbf{u}}$ may be obtained by looking at the spatial evolution of the two systems. The random system evolves much faster initially and quickly loses memory of its initial configuration in the $x-y$ projection while becoming diffuse for times beyond $t = 1.2 - 1.6$ and starts to puff up in the z-direction (Fig. 3) thus evolving to a more isotropic state. However since it is becoming more diffuse it now takes longer to evolve because its density is decreasing.

On the other hand, the rotating system keeps its shape almost perfectly intact until $t = 2$ when a distinctive 4 armed clustering pattern (Fig. 4) starts to appear accompanied by

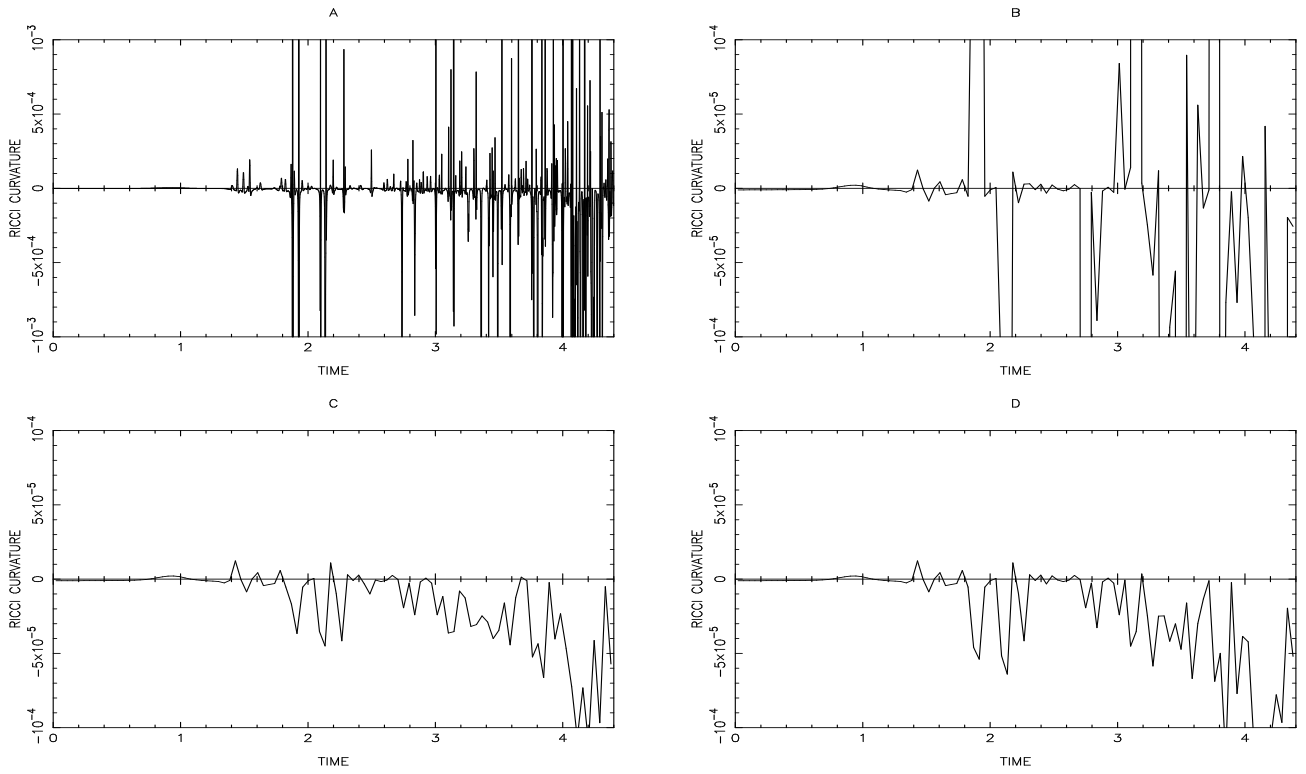

Fig. 1. Ricci curvature time series for rotating "main model" $Scale = 1$ system: **A** Unaveraged time series, **B** with averages taken over a hundred intervals, **C** as in **B** but with a "filter" of 2×10^{-4}, **D** as in **B** but with a filter of 4×10^{-4} and 10×10^{-4} (dotted line)

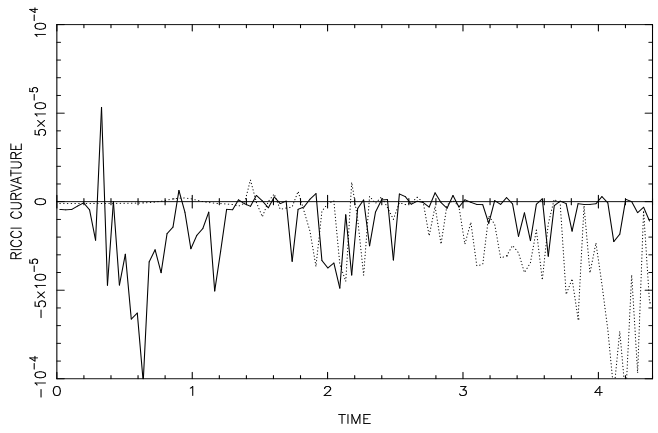

Fig. 2. Ricci curvature time series for main model with random initial x-y velocities and $scale = 1$ (solid line) averaged as in the plot in Fig. 1 C (reproduced here by the dotted line)

the formation of high density areas. This explains the large negative values of the Ricci curvature which in this case represents the collective instability. Since geodesic instability, as stressed earlier, is independent of the particular evolutionary phenomenon in question, this type of relaxation is also included in the description. When one interprets relaxational phenomena in terms of thermodynamic "more probable states" therefore, it should be clear that those types of instabilities could also occur. If they do not lead to complete detachment of a system into components however, the picture that emerges, is that while these phenomena may be important for systems for which the classical theory holds, they cannot characterize the long term evolution of a generic system and that these inhomogeneities themselves produce chaos and evolution towards more probable states under small dissipative or conservative perturbations (Pfenniger & Norman 1990; Hasan et al. 1993; Pfenniger & Friedli 1991; Friedli & Benz 1993; Zhang 1996). They are therefore not typical properties of gravitational systems but transient ones. That, roughly speaking, means that regions of phase-space where this type of instability occurs should be small compared with those where the instability leading to more isotropic states arises.

We now calculate a rough evolutionary time-scale corresponding to the plots in Fig 2. We take it to be *the average exponentiation rate for small random perturbations normal to the phase-space path of the N-body systems*. From the considerations of Section 2.2 this is given by

$$\tau_e \sim \left(\frac{3N}{-2\bar{r}_{\mathbf{u}}}\right)^{1/2} \times \frac{1}{\bar{W}}, \tag{28}$$

where a bar denotes a time average. Now, $r_{\mathbf{u}}$ averages to about -10^{-5} over the whole interval (for both systems) while W starts at a value of 22 but then rises to about 42, therefore we take a value of 30 as a rough mean. This gives a mean exponentiation time-scale of about 200 units—or $0.4\tau_D$ over this period of time (0 to $4.4\tau_D$).

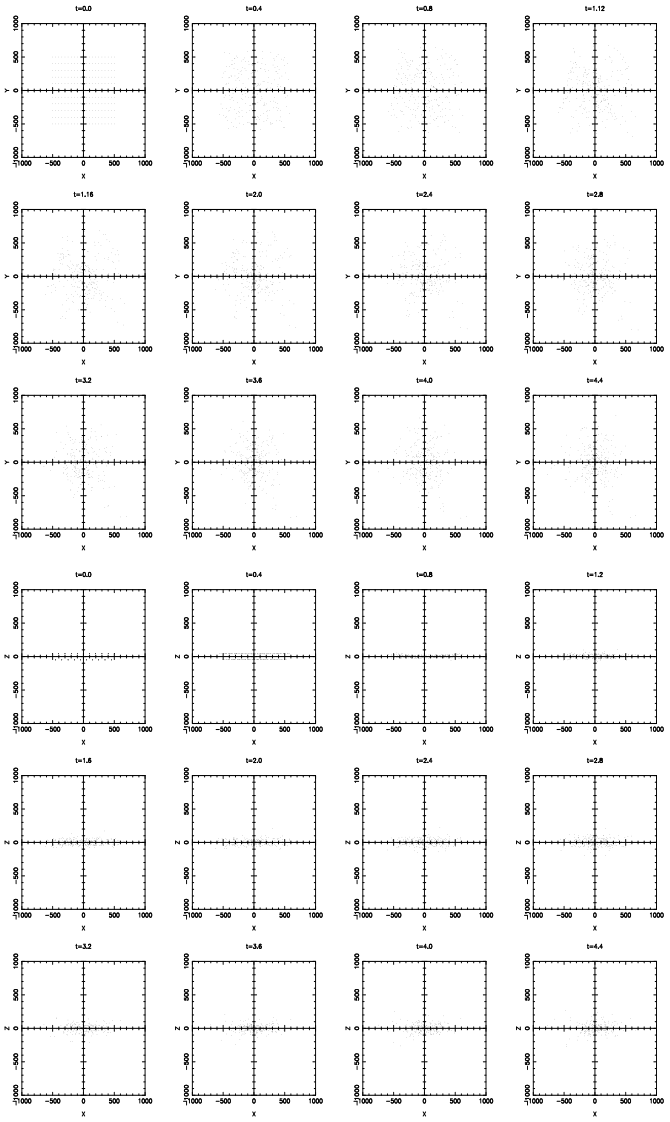

Fig. 3. Spatial evolution of the model corresponding to solid line plot in Fig. 2

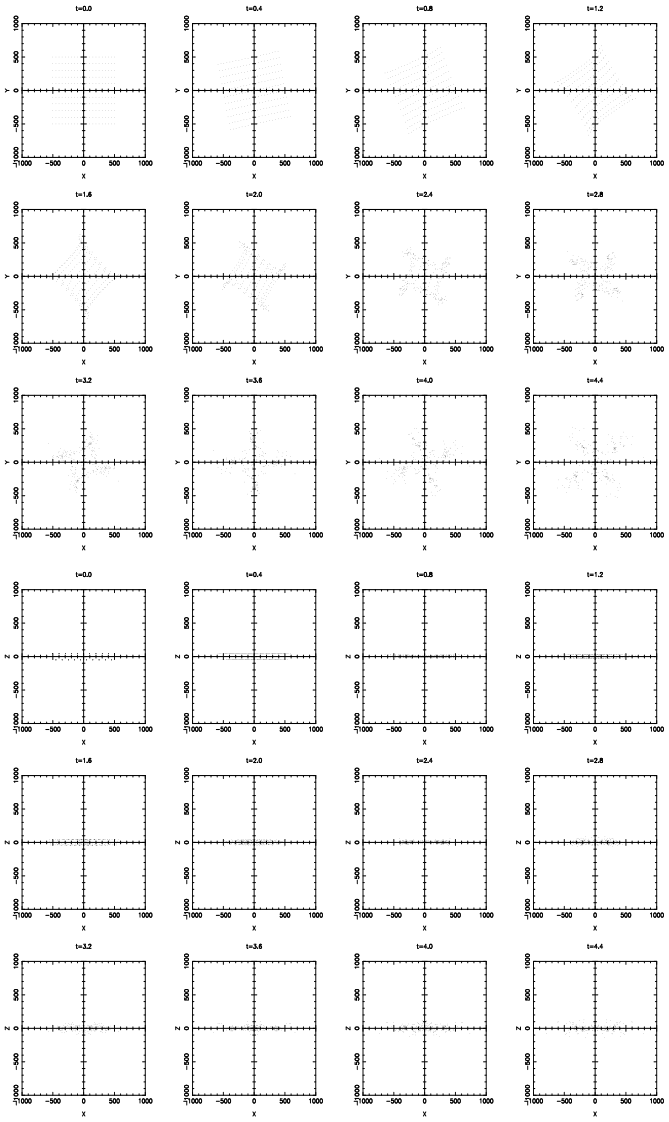

Fig. 4. Spatial evolution of the model corresponding to the dotted line plot in Fig 3

Now, what does this time-scale mean? To answer this question it is important to remember that while the exponential solutions are local and arise from a linearization of the dynamics, this instability exists everywhere because of the negativity of the average of the Ricci curvature. Moreover, the instability is that of the flow in the full $6N$ phase-space and not just particle orbits. Under these conditions, the divergence will probably lead to mixing and filamentation which will radically alter the local structure of the $6N$ phase-space (as mapped by an arbitrary initial partition of that space). Up to resolution ϵ, the phase-space will be completely modified after a time apparently given by (e.g., GS):

$$\tau_\epsilon = \ln \epsilon^{-1} \tau_e. \tag{29}$$

For a numerical application in double precision the smallest resolution available is $\epsilon \sim 10^{-14}$ (incidentally, this number is not too different from the ratio of the size a star to that of a galaxy) so that after a time

$$\tau_\epsilon \sim 32 \tau_e \tag{30}$$

there is complete change in the system's phase-space for all practical purposes. For an ensemble of trajectories having the same energy and integrated independently in a fixed potential, Merritt & Valluri (1996) found that complete mixing did indeed occur over a number of exponentiation time-scales (measured by Liapunov exponents in their case) comparable to that given by (30).

Examples of systems that were proved to behave in this manner include the general class of C-systems (e.g., Arnold's famous cat map: LL). Although we cannot claim that the process is as rigorous in our case, with its non-compact phase-space and sign indefiniteness of the 2d curvatures, we will follow the

assumption that it is at least qualitatively similar (the negativity of the averaged Ricci curvature, the results of GS and Kandrup 1990a,1990b suggest that this may be so). In that case, we have complete modifications of our systems on a time-scale of about 13 dynamical times. Obviously, our two examples have evolved significantly over a time-scale of this order of magnitude — albeit each in different ways and non-uniformly in time. We shall see in Section 4.4 that on a time-scale of $12\tau_D$ there is indeed complete modification for one similar system.

Finally we note that formula (2) predicts an exponential time-scale of about $1.1\tau_D$ which is somewhat larger than the one derived from the Ricci curvature but within reasonable bounds considering it is only an order of magnitude estimate derived for infinite systems and does not take into account effects due to the large scale gravitational field (see Kandrup 1989,1990b) that lead to the clustering in the rotating case for example.

4.3. Varying the energy and virial ratio

We now consider systems with lower densities while keeping the angular momefinger ntum constant. For systems initially in a state of collapse ($vir < 1$) this amounts to varying the energy — making it larger. For these systems, the initial virial ratios (and hence the velocities) is very small, therefore the results for the rotating systems are more or less similar to those for systems starting with random X-Y velocities. We will therefore focus on the latter type only.

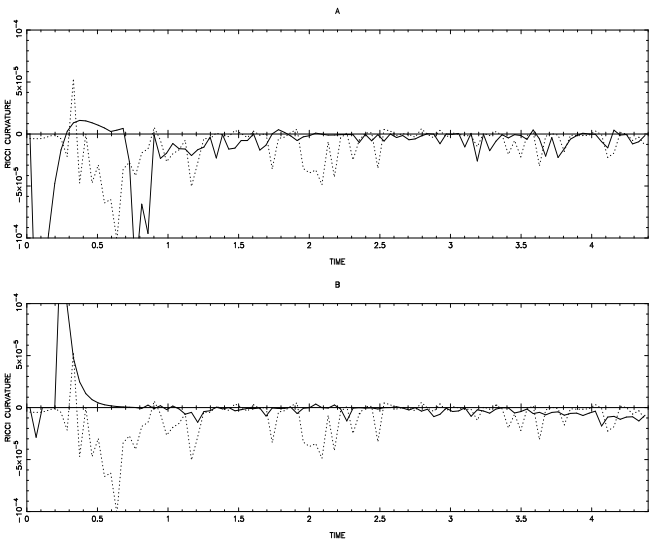

Fig. 5. Ricci curvature time series for random main model systems with: **A** $Scale = 10.8$, **B** $Scale = 100$ averaged as the plot in Fig. 1**C** (reproduced here by the dotted lines)

In Fig. 5 we compare the Ricci time series for initial conditions with $Scale = 10.8$ (Fig. 5A) and $Scale = 100$ (Fig. 5B) (shown by the solid lines) with those of the $Scale = 1$ (dotted line). Clearly, there is a trend towards larger time-scales of evolution for the less dense systems, especially if one takes into account that the ratio of the kinetic energy W at virial equilibrium of the $Scale = 1$ system to that of the $Scale = 10.8$ and the $Scale = 100$ systems is 7.3 and 65.9 respectively. These results may seem counterintuitive since one knows that for initial conditions far from dynamical equilibrium there is a well known instability at work — namely violent relaxation. The confusion is resolved however when one notices that the dynamical time for these two systems is much larger than the original — being 35.49 and 1000 times larger. Thus, based on the above considerations, we expect a system characterized by the Ricci curvature shown by the solid line in Fig. 5B to evolve extremely slowly in "physical" time units but relatively fast, compared to the one shown by the dotted line, in terms of dynamical time. The fact that the kinetic energy varies rapidly along the motion prevents us however from calculating any precise estimates.

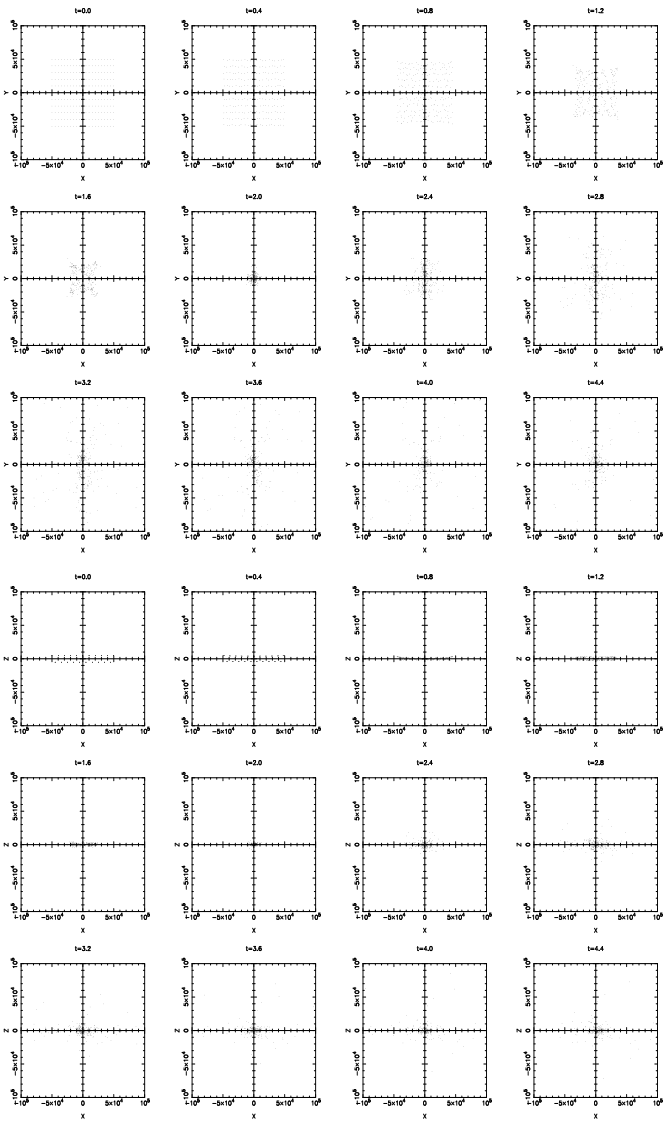

Fig. 6. Spatial evolution of the model corresponding to the solid line plot in Fig. 5 **B**

By looking at Fig. 6 one can clearly see that this is the case. With every interval between "snapshots" in this figure corresponding to a thousand intervals in Fig. 3 one sees that the

$Scale = 100$ system evolves much more slowly in physical time. In terms of intrinsic dynamical times however, it is clear that it evolves much faster than the $Scale = 1$ system; having quickly lost all trace of its initial spatial configuration it then appears to be evolving towards a state characterized by an increasingly tight core and diffuse "halo". At this stage one notices, the almost constant (drifting slowly towards lower) negative values of $r_{\mathbf{u}}$ in fig 5B (solid line) beyond $t \sim 3$, showing that the system is becoming more and more mixing, in agreement with discussion in section 3.1.

4.4. Systems starting in virial equilibrium

We now keep the energies constant and increase the angular momenta of the rotating systems in such a way as to have virial equilibrium in the initial state. This will be accompanied by contraction in the scale of the system. For example, the $Scale = 100$ equilibrium models will have an inter line spacing of about half that of the main models with the same energy. The systems with random $x - y$ velocities start from the same spatial configurations as the rotating ones and with the absolute values of the velocities rescaled accordingly.

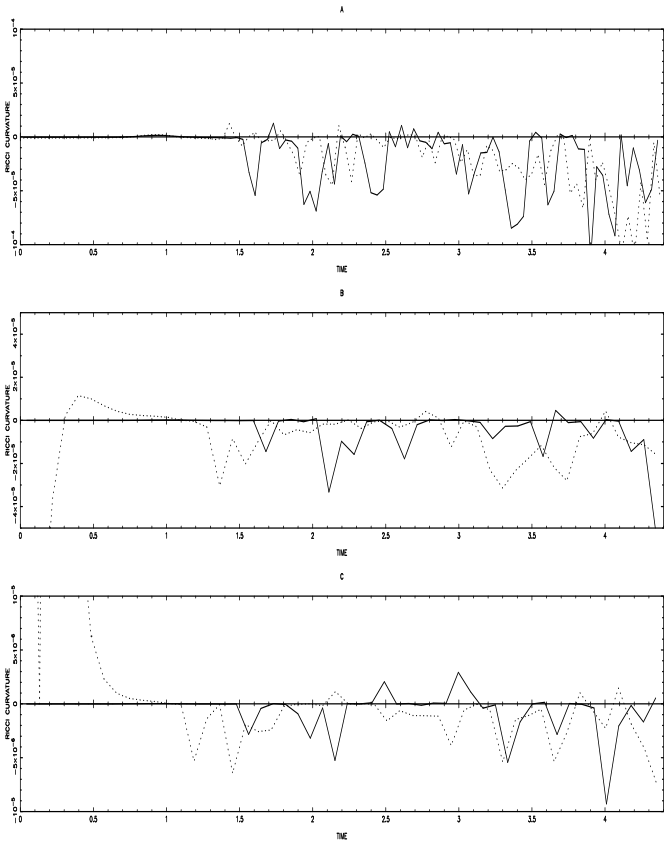

Fig. 7. Ricci curvature time series for random main model systems with: **A** $Scale = 10.8$, **B** $Scale = 100$ averaged as the plot in Fig. 1**C** (reproduced here by the dotted lines) Ricci curvature time series of the rotating equilibrium models (solid lines) compared with the main (collapsing) models: **A** $Scale = 1$, **B** $Scale = 10.8$, **C** $Scale = 100$. In **B** and **C** averages are taken over 50 time intervals (instead of a 100)

For a system in a steady state we expect $r_{\mathbf{u}}$ to be constant in time. If, in addition, the motion is regular (e.g., our sheets rotate rigidly) we expect $r_{\mathbf{u}}$ to be very near zero. Nevertheless, due to the differential rotation which is accompanied by collective instability and clustering, this state of affairs cannot last too long. Similarly, due to the instability of the initial state in the random case, the early equilibrium is lost. These considerations are confirmed by plots of the Ricci curvature (Fig. 7) where values for the equilibrium cases (solid lines) are compared with those of main models of the same energies (dotted lines). Although the curvature is still negative even at early times, the evolution time-scale given by Eq. (30) is now about 70 dynamical times. It also is immediately apparent that the more distant the original system was from virial equilibrium the bigger the difference of its initial behaviour from its equilibrium counterpart. For example, for the $Scale = 1$ system (Fig 7A) the dotted and solid lines are almost indistinguishable, while for the other two systems the contrast in the early evolution is much clearer. Later on however, non-equilibrium systems quickly tend towards virial equilibrium, making the contrast weaker. (The reason for the positive bumps in the time evolution of the curvature for these models is that, despite the fact that we average over 50 time intervals, the irregularities cannot be suppressed because the filtering is too large the fluctuations now are much smaller because of the lower density.) It is clear from these graphs that, because the dynamical time of the equilibrium systems is smaller than the collapsing ones (about a third for the $Scale = 100$ models), the equilibrium models actually evolve slower than the collapsing systems in terms of intrinsic dynamical times throughout most of the evolution. From that, and from the results of the previous subsection, we conclude that systems starting from a state of collapse are possibly more unstable than ones starting near virial equilibrium. The difference does not however appear to be very large.

The $x-y$ spatial evolution in time of the rotating $Scale = 100$ equilibrium model is shown in Fig. 8 where the integration was carried over a time interval corresponding to the physical time of integration of its main model counterpart with same energy. It is clear that by $t = 4.48$ the clustering is at least as pronounced as in Fig. 4 at $t = 4.4$ (a similar comparison can be made with the corresponding equilibrium model which behaves in a very similar manner). This is not surprising given the scale free nature of gravitational interactions. It is therefore interesting to see what the rough time-scales derived from the Ricci curvature might tell us about this apparent coincidence. Let us label the quantities relating to the $Scale = 1$ equilibrium initial state by indices 1 and those relating to the $Scale = 100$ equilibrium system by 100 . The ratios of the two evolutionary time-scale are then

$$\frac{\tau_{100}}{\tau_1} = \sqrt{\frac{\bar{r}_{\mathbf{u}1}}{\bar{r}_{\mathbf{u}100}}} \frac{\bar{W}_1}{\bar{W}_{100}} \frac{\tau_{D1}}{\tau_{D100}}. \tag{31}$$

Both systems are always near virial equilibrium throughout the evolution therefore the W's are constrained to be near values given by $W = -E$ so that $\bar{W}_1 \sim 41.53$ and $\bar{W}_{100} \sim 0.63$, the averages $\bar{r}_{\mathbf{u}1}$ and $\bar{r}_{\mathbf{u}100}$ are calculated over the interval $t = 0$ to $t = 4.4$ to be $\bar{r}_{\mathbf{u}1} = -1.6 \times 10^{-5}$ and $\bar{r}_{\mathbf{u}100} = -5.8 \times 10^{-7}$. Finally

$$\frac{\tau_{D100}}{\tau_{D1}} = \left(\frac{d_{100}}{d_1}\right)^{3/2} = (50.17)^{3/2} = 355.41, \tag{32}$$

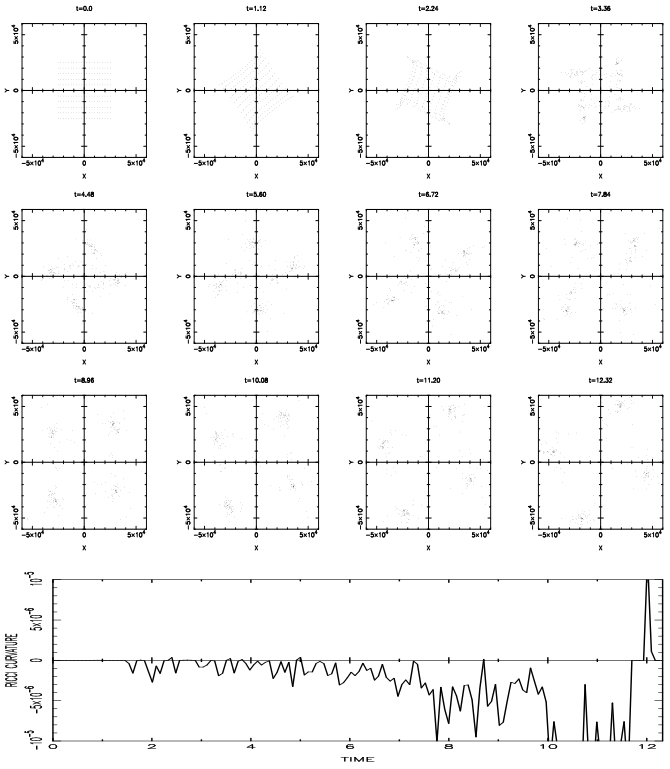

Fig. 8. Longer time behaviour of the Ricci curvature and the corresponding x-y projection of the spatial evolution for the system corresponding to the solid line plot in Fig. 7C. Filtering is taken equal to 2×10^{-5} and averaging is done over 150 intervals.

where d_1 and d_{100} are the initial separations of adjacent particles on the sheets. Inserting these numbers we get

$$\frac{\tau_{100}}{\tau_1} = 0.97. \tag{33}$$

Now, considering that the systems differ radically in energy, angular momentum and dynamical time-scales this result is rather impressive—especially if one recalls the rough way in which we have averaged and filtered the data. It may be useful to note that Eq. (2) predicts the same behaviour, we have

$$\tau_{gs} \sim \frac{W^{1/2}}{n^{2/3}} \sim \frac{W^{1/2}}{n^{1/6}} \tau_D \sim (Scale \times W)^{1/2} \tag{34}$$

which gives

$$\frac{\tau_{gs100}}{\tau_{gs1}} = 0.87. \tag{35}$$

Looking at the longer time behaviour in Fig. 8 we see that the clustering continues leading to almost total separation of the components. The corresponding behaviour of $r_{\mathbf{u}}$ is also shown. As would be expected, the clustering gives rise to shorter evolutionary time-scales. Three characteristic time-scales can be isolated: from $t = 0$ to $t = 7$ the system can still be considered to be one part and is connected until $t \sim 10$ but then detaches after that. These stages are clear from Fig. 8 . Thus there is complete modification of the initial state after about 12 dynamical times as expected from Eq. (30). To illustrate how the results depend on filtering, we have chosen a filtering here of 2×10^{-5} instead of the value 2×10^{-4} usually used. Hence the smoothness of the time series up to $t = 4.4$ in comparison with the one in Fig. 7C. The positive bump on the right is due to the filtering becoming too small relative to the absolute value of $r_{\mathbf{u}}$ so that the value in this last interval has little statistical significance.

Similar results are obtained for the cases with random initial $x - y$ velocities. Here, the formula for two body relaxation for a Maxwellian distribution (BT formula 8.71 which is more or less appropriate in this case) gives a ratio of $\tau_{100}/\tau 1 = 0.87^3 = 0.66$ for these two cases.

4.5. The effect of softening

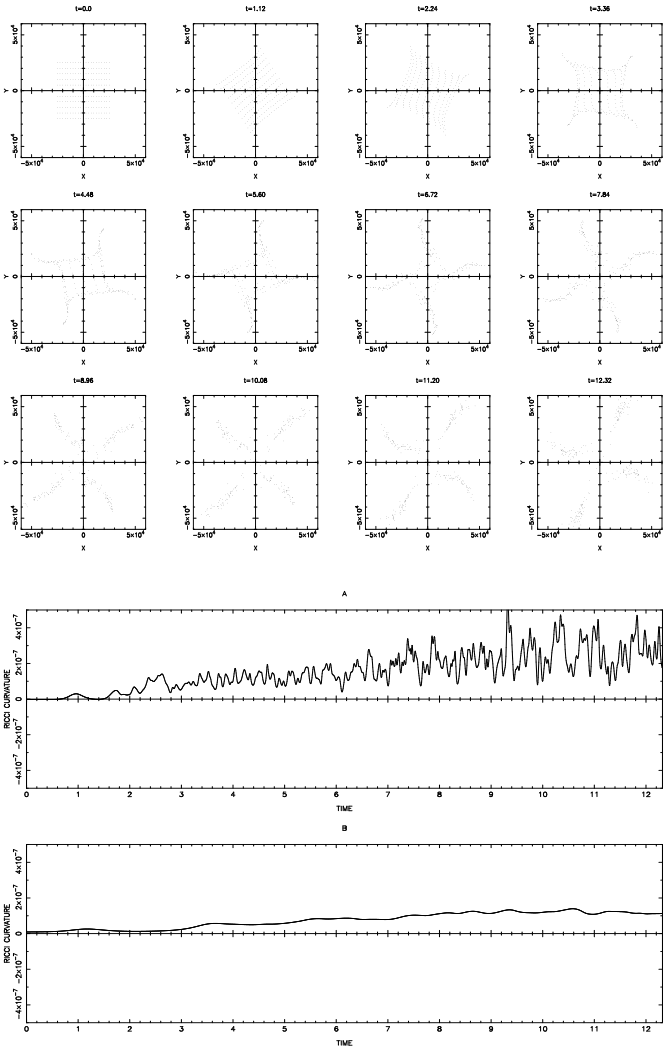

Fig. 9. The effect of softening: Same as in Fig. 8 but when the force law is softened: **A** When the softenening radius is equal to 10% the inter-particle distance on the same line, **B** same as in **A** but when the softening radius is equal to 80% the initial inter-particle distance on the same line. The $x - y$ coordinate evolution (top) correspond to the system in **B**

Fig 9A shows the un-averaged Ricci time series for a system starting with the same initial conditions as the one in Fig. 8 but when the potential contains a softening parameter (BT formula 2.194) of 10% the initial separation between particles in the same line, while Fig. 9B shows the the evolution of $r_{\mathbf{u}}$ for the same system but when the softening radius is about 80% of the original separation between particles in the same line. First, one notices the absence of large fluctuations in the value of $r_{\mathbf{u}}$. This is to be expected since formula (23) no longer contains singularities at close encounters. The second and more fundamental effect however is that the Ricci curvature is now positive. This is due to the fact that the last term on the right hand side is now non-zero and is always positive since it corresponds to the density. For small softening (say 1% of inter-particle distance) the original behaviour of $r_{\mathbf{u}}$ is recovered, however as the softening increases this term becomes large. In addition, the second term in (23), which in general gives a highly fluctuating contribution the average of which is small, starts becoming positive too.

The above means that *in the presence of significant softening, N-body gravitational systems no longer approximate the uniformly hyperbolic Anosov C-systems* because the Ricci curvature is no longer negative on average. That is, there is a fundamental change of structure in the phase-space of N-body systems when softening is introduced. Therefore if one takes the view that a softened N-body system is an approximation of the continuum formulation of a problem, one must realize that this formulation has solutions which can behave in a different manner from those of a discrete system. Indeed it was found that the evolution of the softened systems differed considerably from the un-softened ones. For example in Fig. 9 we also show the $x-y$ evolution from the same initial conditions as in Fig. 8 but when a softening parameter of 80% the original separation of particles is present in the force law. Instead of the clustering pattern that was obtained in the un-softened case, there is now a type of filamentary structure taking its place and the system never completely detaches into components. (In fact when the simulation is continued these filaments are destroyed and one gets a nearly isotropic system.) Although this system is still unstable, the dominant mechanism of instability is likely to be different. It was observed for example that while in the un-softened system the virial ratio stays close to 1, in the softened case it departs significantly from that value, being less than 1 for the time-scale of the plot then increasing significantly later. This may suggest that the mechanism of instability here is a parametric instability related to that effect (Cerruti-Sola & Pettini 1995). For systems with intermediate softening a mixture of different mechanisms could be present. When the negativity of the curvature is dominant, a system approximates a discrete one. This criteria may be useful in choosing softening parameters (or laws) in numerical simulations that eliminate the effect of close encounters but do not qualitatively change the results.

The difficulty we are encountering here however is a fundamental one. As long as the system we are considering is discrete and direct collisions are negligible the offending term in Eq. (23) is zero and the Ricci curvature is likely to be negative. As mentioned in the introduction and in the beginning of section 2.3, this is even more likely to be the case as N increases. On the other hand the smoothing of the density distribution leads to positive curvature. The structure of the phase-space (which is the cotangent bundle of the configuration manifold the curvature of which we are calculating) in the two cases is then presumably radically different. This suggests that *it is not obvious that large-N but discrete systems are well approximated by the continuum limit* even if the discreteness noise in the force decreases as N increases. There appears to be a type of "phase transition" in the structure of the $6N$ phase-space when passing from one limit (large-N but discrete system) to the other (continuous system). This is the same conclusion we were led to from the general considerations of the introduction.

Obviously these issues will require much more thorough investigation which is beyond the scope of this exploratory paper. We will however briefly comment on this problem from the perspective of the scalar curvature which we now discuss.

4.6. Scalar curvature

When the two dimensional curvatures are averaged over all geodesics that originate at a point of M as well as all possible directions normal to the geodesics, one obtains the curvature scalar

$$R = \sum_{\mathbf{u},\mathbf{n}} k_{\mathbf{u},\mathbf{n}} = \sum_{\mathbf{u}} r_{\mathbf{u}}. \tag{36}$$

With the quantity $R/3N(3N-1)$ replacing $r_{\mathbf{u}}/(3N-1)$ in Equation (22) one can define a corresponding instability criterion and an associated time-scale. This is obviously a more drastic approximation, and because R will not depend explicitly on the velocities (since we have summed over the directions in the tangent space TM) it cannot contain generic information about a system and its use for short time characterization of the dynamics can be especially dangerous (e.g., Cipriani & Pucacco 1994). Nevertheless, the similarity of the third term in the formula (23) for the Ricci curvature to the expression for R (GS formula (27)) suggests that when this term is dominant, the scalar curvature may give a reasonable description of the dynamics. The fact that estimates of evolutionary time-scales resulting from the order of magnitude formula of GS agreed within reasonable bounds with the ones obtained from the computations of $r_{\mathbf{u}}$ suggests that this term may be important in some cases since that formula is based on an estimate of the scalar curvature.

To see if this is true, we have computed the scalar curvatures along the motion of the systems described in the previous sections. We have found that using a hundred averaging intervals and filtering equal to twice the absolute value of the maximum scale in the figures gives reasonably smooth time series for R that do not sensitively depend on the averaging and the filtering threshold used. Fig. 10 shows the resultant time series for the rotating equilibrium models. Clearly, those results agree qualitatively with those inferred from the behaviour of the corresponding time series for $r_{\mathbf{u}}$ in Fig. 7 (although differing in some detail). The time-scales also agree (when R is divided by $3N(3N-1)$ as described above). This agreement is because out of the three non-zero terms in Eq. (23), the first is small unless the velocity vectors of particles are almost aligned with their acceleration vectors and the second is highly fluctuating and averages to very small values (this is because it describes the variations of the force at the particle positions which, as one would expect, depends sensitively on the position of close neighbours). This leaves the third term which is the one that appears in the formula for the scalar curvature.

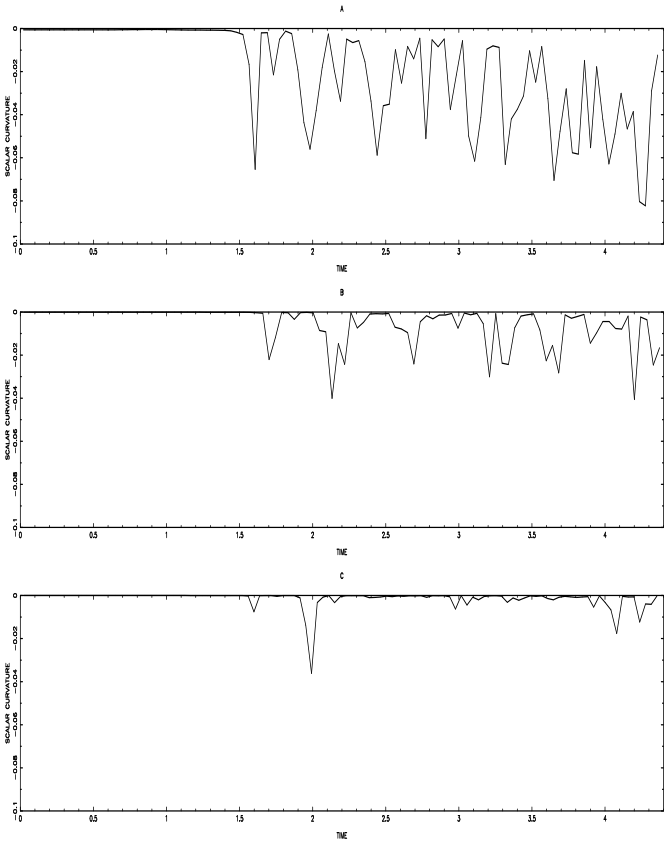

Fig. 10. Scalar curvature for the rotating equilibrium models **A** $Scale = 1$, **B** $Scale = 10.8$, **C** $Scale = 100$

The scalar curvature — like the Ricci curvature — also takes positive values when significant softening is used. As was noted in the introduction, the continuum approximation with a steady state potential reduces the N-body problem to N one-particle problems in a given potential. In this context, the above discrepancy between the value of the curvatures of softened and un-softened cases may perhaps be understood by noticing that the scalar curvature for $N = 1$ is *always* positive no matter what the potential is (assuming positive density). The 6-dimensional phase-space is therefore far from approximating a hyperbolic structure like that of C-systems. Even in this case, chaos may still occur (some two dimensional curvatures may still be negative and there is also the possibility of parametric instability: ARN; P93) but it will not likely be as robust or widespread as in systems with negative curvature.

5. Conclusions

The assumptions of classical non-evolutionary galactic dynamics may not be satisfied in the presence of significant amount of chaos (section 1). This makes it important to develop and to test methods characterizing such chaotic behaviour. Geometric methods have the double advantage of being *local* and comparing *normal* deviations between trajectories of dynamical systems and not the total divergence of temporal states. For higher dimensional systems these properties may be important in distinguishing between true phase space mixing which can be accompanied by changes in the physical characteristics of a system and phase mixing which conserves the action variables. Geometric methods are therefore better suited for studies of the short time evolution of galaxies than other (more traditional) measures of chaos (section 2 and 3.1).

In large dimensional systems it may not be practical to determine the stability of a trajectory to all possible perturbations. The next best thing is to determine the average divergence of trajectories due to random perturbations. One way of doing this is by examining the Ricci curvature of the Lagrangian configuration manifold of a dynamical system (section 2.3). To check the effectiveness of such an approach for N-body gravitational systems we have calculated the Ricci curvature for several small N-body systems integrated with high precision (section 3.2 and 4). The results of these experiments show that:

1. When properly averaged to get rid of the contributions of close encounters the Ricci curvature is almost always negative, confirming that gravitational systems are unstable (e.g., Miller 1964; Goodman et al. 1993; Kandrup et al. 1994) and that the main mechanism of instability is the negativity of the curvature of the configuration manifold as predicted by Gurzadyan & Savvidy (1984,1986) and Kandrup (1990a,1990b).
2. The Ricci curvature is more negative (hence predicts shorter evolutionary time-scales) when a system develops pronounced macroscopic instabilities (e.g., plasma type collective instabilities). In this case the rates of spatial macroscopic evolution of the different systems both relative to each other and in terms of evolution time-scales was reasonably well described by the time-scales derived on the basis of the Ricci curvature calculations.
3. When expressed in terms of dynamical times, evolutionary time-scales appeared to be slightly longer for systems starting from virial equilibrium than those starting from a virial ratio less than one. However, since when the kinetic energy varies significantly, chaotic behaviour cannot be described by the negativity of the Ricci curvature alone (Cerruti-Sola & Pettini 1995) this conclusion remains to be confirmed. (However in the case of large N-body systems near virial equilibrium the objections to the use of the Ricci curvature as outlined in the aforementioned paper are not likely to be important since the second and third term of their Eq. (26) are then very small. By using the Ricci curvature and eliminating large fluctuations due to close encounters we have therefore implicitly assumed that it is the instability in that (large-N) limit that interests us and not effects due to small scale fluctuations.)
4. In the presence of significant (but not very large) softening, the Ricci curvature becomes positive. This probably means that the phase-space structure of softened systems is radically different from that of point particles. This has consequences for the interpretation of results of numerical simulations. More fundamentally however this result may be interpreted to mean that *there is no continuous transition from large-N discrete N-body systems to continuous ones*. It may therefore explain why large N-body spherical systems are found to approximate exponentially unstable C-systems while it is known that motion in smooth spherical potentials is separable. More work however is needed to

fully understand the meaning of this effect and its possible consequences.

5. Results derived on the basis of the scalar curvature agreed, in general, with those obtained from the evolution of the Ricci curvature. This shows the instability to be quite a robust phenomenon.

We have not looked at properties such as energy relaxation here. As was mentioned in the introduction this can have different time-scales from that of the instability of trajectories. To see how this may be the case we consider the change in the Hamiltonian $H = T + V$ of a test particle i in an N-body system. Using the Hamiltonian equations we find that along the motion this is given by

$$\frac{dH_i}{dt} = \frac{\partial H_i}{\partial t} = \frac{\partial V_i}{\partial t} \tag{37}$$

with the interaction potential V_i given by

$$V_i = \sum_j V_{ij} \tag{38}$$

being a function of the positions of the remaining $N-1$ particles which are of course time dependent functions of the initial conditions. The change in energy of particle i along its path is then given by

$$\int \frac{\partial V_i}{\partial t} dt = \int \sum_j \frac{\partial V_{ij}}{\partial t} dt = \sum_j \int \frac{\partial V_{ij}}{\partial t} dt, \tag{39}$$

which is the sum of the energy changes due to the individual interactions and therefore could proceed on time-scales similar to that given in (1). This does not of course mean that energy relaxation cannot be enhanced for systems consisting of particles with different masses or those out of virial equilibrium or where collective motion or large scale inhomogeneity or anisotropy occurs. In these cases chaotic behaviour can be important for energy relaxation. Indeed there is some evidence that in some situations two body relaxation estimates are inaccurate even for energy relaxation (El-Zant 1996a). In general however there may be phase-space "barriers" across which diffusion is slow. This may prevent some quantities from relaxing even when chaos is present (discussions of the issue of phase-space transport in higher dimensional Hamiltonian systems can be found in Wiggins 1991 or Benettin 1994). Nevertheless, chaos implies exponential divergence *normal* to the phase-space trajectory leading to diffusion in at least some of the action variables which determine the physical characteristics of a system (as opposed to phase mixing which conserves the action variables). It therefore has important consequences for the behaviour of dynamical systems as was stressed in the introductory section of this paper. This has long been generally recognised in various branches of Physics and Mathematics (e.g., Sagdeev et al. 1988) but not always in stellar dynamics. The question therefore is *how widespread is the chaotic behaviour in realistic N-body realizations of the different galaxy types and what are the exponentiation time-scales.* This is what we hope to find out using the method examined in this paper.

Acknowledgments

I would like to thank Prof. R.J. Tayler for constructive comments on an earlier version of this paper, Prof. V.G. Gurzadyan for enlightening discussions and some important suggestions, Simon Goodwin for helping me with the English and the referee Daniel Pfenniger for comments that helped improve the presentation. I would also like to thank Henry Kandrup for a useful discussion that helped clarify some of my ideas on the subject of this paper and Douglas Heggie for helpful communication. This work was undertaken while the author was supported by a Foreign and Commonwealth Office Chevening scholarship.

References

Abraham R., Marsden J.E., 1978, Foundations of Mechanics. Benjamin, Reading, Massachusetts

Anosov D.V., 1967, Geodesic Flows on Closed Riemann Manifolds with Negative Curvature. Proceedings of the Steklov Institute of Mathematics: 90

Arnold V.I., 1989, Mathematical Methods of Classical Mechanics. Springer Verlag, New York (ARN)

Benettin G.,1994, Prog. Theo. Phys. Suppl. 116, 207

Binney J., 1982, Dynamics of hot stellar systems. In: Binney J., Kormendy J., White S.D.M. (eds.) Morphology and Dynamics of Galaxies. Geneva Observatory, Sauverny

Binney J. & Tremaine S., 1987, Galactic Dynamics. Princeton Univ. Press, Princeton (BT)

Braun W., Hepp K., 1977, Commun. Math. Phys. 56, 101

Casetti L., Pettini M., 1993, Phys. Rev. E48,4320

Cerruti-Sola M., Pettini M., 1995, Phys. Rev. E51, 53

Cipriani P., Pucacco G., 1994, Il Nuovo Cimento 109B, 325

Courteau C., de Jong R.S., Broeils A.H., 1996, ApJ in press

Eckmann J.P., Ruelle D., 1985, Rev. Mod. Phys. 57, 617

Eisenhart L.P., 1926, Riemanian Geometry. Princeton Univ. Press, Princeton

El-Zant A.A., 1996a, Stability of motion of N-body gravitational systems. In: Chaos in Gravitational N-body Systems, Muzzio J.C. (ed). Kluwer

El-Zant A.A., 1996b, Ph.D. thesis, University of Sussex

Friedli D., Benz W., 1993, A&A 268, 65

Gerhard O.E., 1985, A&A 151, 279

Goldstein H., 1980, Classical Mechanics. Addisson-Wesley

Goodman J., Heggie D.C., Hut P., 1993, ApJ 415, 715

Gurzadyan V.G., Savvidy G.K., 1984, Sov. Phys. Dokl. 29, 520

Gurzadyan V.G., Savvidy G.K., 1986, A&A 160, 203 (GS)

Gurzadyan V.G., Kocharyan A.A., 1987, Ap&SS 135, 307

Gurzadyan V.G., Pfenniger D., 1994, Ergodic Concepts in Stellar Dynamics. Lecture Notes in Physics 430, Springer Verlag, New York

Gurzadyan V.G., Kocharyan A.A., 1994, Paradigms of the Large-Scale Universe. Gordon and Breach, New York

Hasan H., Pfenniger D., Norman C.A., 1993, ApJ 409, 91

Hernquist L., Ostriker J.P., 1992, ApJ 386, 375

Hertz H., 1900, The Principles of Mechanics Presented in a New Form. Macmillan Company. Reprinted by Dover Publications, New York in 1956

Kandrup H.E., 1989, Phys. Letters A140, 97

Kandrup H.E., 1990a, ApJ 364, 420

Kandrup H.E., 1990b, Physica A169, 73

Kandrup H.E., 1994, invited talk at seventh Marcel Grossman meeting July 1994 (astro-ph/9410091)

Kandrup H.E., Mahon M.E., Smith H., 1994, ApJ 428, 458

Krylov N.S., 1950, Studies on the Foundation of Statistical Physics. Publ AN SSSR, Leningrad. Eng. trans. Princeton

University Press. 1980
Lichtenberg A.J., Lieberman M.A., 1983, Regular and Stochastic Motion. Springer Verlag, New York (LL)
Lynden-Bell D., 1972, Elementary statistical mechanics of stellar systems. In: Contopoulos G., Hénon M., Lynden-Bell D. (eds) Dynamical Structure and Evolution of Stellar Systems. Geneva observatory, Sauverny
Mackay R.S., Meiss J.D., 1987, Hamiltonian Dynamical Systems. J.W. Arrowsmith ltd., Bristol
McCauley J.L., 1993, Chaos, Dynamics and Fractals: an algorithmic approach. Cambridge Univ. press, Cambridge
Merritt D., Fridman T., 1996, ApJ 460, 136
Merritt D., Valluri M., 1996, ApJ 471, 82
Miller R.H., 1964, ApJ 140, 250
Misner C.W., Thorne K.S., Wheeler J.A., 1973, Gravitation. Freeman
Nekhoroshev N.N., 1977, Rus. Math. Surv. 32, 5
Pars L.A., 1965, A treatise on Analytical Dynamics. Heinemman, London
Perry A.D., Wiggins S., 1994, Physica D71, 102
Pesin Ya.B., 1989, General theory of smooth hyperbolic dynamical systems. In: Sinai Ya.G. (ed) Dynamical Systems II; Egodic theory. Springer Verlag, Berlin
Pettini M., 1993, Phys Rev. E47, 828 (P93)
Pfenniger D. 1986 A&A 165, 74
Pfenniger D., Norman C.A., 1990, ApJ 363, 391
Pfenniger D., Friedli D., 1991, A&A 252, 75
Pfenniger D., Combes F., Martinet L., 1994, A&A 285, 79
Poincaré H., 1893, Les Méthodes Nouvelles de la Mécanique Céleste. Gautier Villard, Paris (and Dover, New York, 1957)
Pucacco G., 1992, A&A 259, 473
Sagdeev R.Z., Usikov D.A., Zaslavsky G.M., 1988, Nonlinear Physics: from the pendulum to turbulence and chaos. Harwood Academic, New York
Saslaw W.C., 1985, Gravitational Physics of Stellar and Galactic Systems. Cambridge University press, Cambridge
Sellwood J.H, 1987, in: Hut P., McMillan S. (eds.) The Use of Supercomputers in Stellar Dynamics. Lecture Notes in Physics 267, Springer Verlag, Berlin
Udry S., Pfenniger D., 1988, A&A 198, 135
van Albada T., 1987, in: Hut P., McMillan S., (eds.) The Use of Supercomputers in Stellar Dynamics. Lecture Notes in Physics 267, Springer Verlag, Berlin
Whittaker E.T., 1937, A Treatise on Analytical Dynamics. Cambridge Univ. press, Cambridge
Wielen R., 1977, A & A 60, 263
Wiggins S., 1991, Chaotic Transport in Dynamical Systems. Springer Verlag, New york
Wolf J.B., Swift J.B., Swinney A.L., Vastano J.H., 1985, Physica 17D, 288
Zhang X., 1996, ApJ 457, 125

This article was processed by the author using Springer-Verlag LaTeX A&A style file 1990.